Excitation of Global Alfvén Waves by Low RF Power on TCABR

P G P Puglia, A G Elfimov, L Ruchko, R M O Galvão, Z O Guimarães-Filho, G Ronchi, A M M Fonseca, Yu K Kuznetsov, I C Nascimento, A P Reis, W P de Sá, E K Sanada, J H F Severo, V C Theodoro and J I Elizondo

Plasma Physics Laboratory, Institute of Physics at University of São Paulo, São Paulo, Brazil

E-mail: ppuglia@if.usp.br

Abstract. Recent results of Global Alfvén wave (GAW) excited by external antenna and fed by low radio-frequency (RF) power (≤1kW) in tokamak TCABR are presented. The goal of this work is to develop a diagnostic tool based on the excitation of GAW using low power RF generators when the waves can be excited without perturbing the basic plasma parameters in TCABR. This method named MHD diagnostics has already been developed on other tokamaks for toroidicity induced Alfvén eigenmodes as well for GAW. Two magnetic probes are used for measurements of the magnetic field perturbations in two regimes of excitation. In the first one, the fixed RF frequency is combined with gas-puffing induced density rise and relaxation (1-2)×10^{13} /cm^3 in order to meet the GAW resonance, while in the second excitation method RF frequency sweeps 2-4 MHz are applied to the relatively stable plasma density. The plasma discharges are accompanied by saw-tooth (ST) oscillations registered by Soft-X Ray diagnostics that helps in an identification of the GAW resonances due to ST density oscillations. It is found that the fixed frequency GAW resonance appears during density rise, as well during slow density reducing after stop of gas puffing. The effective mass number A_{eff}=1.36 is found.

1. Introduction

Global Alfvén waves (GAW) discovered theoretically [1, 2] and observed experimentally in tokamaks [3, 4] were later proposed to use for diagnostic purpose. This method named as "MHD diagnostics" has already been proposed in [5, 6, 7, 8, 9] to identify the mass number and security factor profile and was tested in other tokamaks for toroidicity induced Alfvén eigenmodes as well for GAW. The basic Alfvén wave (AW) continuum equation is presented as follows:

$$\omega_A = k_{\|} V_A = \frac{B}{\sqrt{\mu_0 n m_H A_{eff}}} \frac{1}{R}\left(N + \frac{M}{q}\right) \quad (1)$$

Here, ω_A is the Alfvén wave frequency, $k_{\|}$ is the wave vector parallel to the magnetic field, V_A is the Alfvén speed, B is the magnetic field strength, n is the electron density, m_H is the hydrogen nuclei mass, A_{eff} is the effective ion mass, R is the major tokamak radius, (N,M) the toroidal and poloidal wave numbers and q the safety factor. Typically, GAW eigenmodes may appear at the extreme points

of the AW continuum to avoid strong continuum dissipation. As we can see in equation (1), the A_{eff} is inversely proportional to the Alfvén frequency in square giving us the possibility to try to estimate that parameter based on the identified GAW frequency, density profile, mode numbers and consideration of q profile.

In this work, we are going to use the excitation of Global Alfvén waves as a diagnostic tool to identify mass number in TCABR. The machine has the following main parameters: major radius R_0 = 0.615m, minor radius a = 0.18m, toroidal magnetic field $B0$ = 1.07T, plasma current IP ≈80- 85kA, line averaged electron density $\bar{n}$= 1.2– 2.4×$10^{19}$$m^{-3}$, and central electron temperature T_{e0}≈430-480eV, in the discussed ohm discharges. We find that the typical plasma, which is similar to the old TCA [10], stays in a mixed state of diffusion, a plateau diffusion for the hydrogen ions and electrons and Pfirsch-Schlüter regime for the impurities, that may cause an accumulation of impurities on the plasma core [11] changing the electronic density profile. If we assume a parabolic profile for the impurity free plasma, we end up with a density profile in the form [11]

$$n_e = n_{0H}(1 - r^2/a^2)^{\alpha} + n_{0Z} e^{-\frac{r^2}{(0.4a)^2}} \quad (2)$$

Where n_{0H} is the hydrogen density at the plasma center, a is the plasma minor radius, r the radial position, α a profile parameter and n_{0Z} the impurity density at the plasma center. The impurity accumulation creates a higher density on the plasma core, so we can expect a higher value for the effective ion mass on the center of the plasma because of the impurity accumulation.

Contrary to previous high RF power experiments [12], it is proposed to apply the low power (≤1kW) of RF generators to excite waves without disturbing the basic plasma parameters. Here, we are more concerned about the identification of the Alfvén waves, to perform an estimate of the plasma ion effective mass, and the ions relative concentration. The results presented in this paper are only a rough estimate and will be more explored in future work. The GAW excitation is proposed in the TCABR conditions with sawtooth oscillation when q-value at center is near to one. For monotonic q-profile typical for TCABR, the GAW eigenmodes may be exited at the plasma core for the toroidal modes N≥2. By identifying the frequency of excited waves and their mode numbers, therefore, it is possible to obtain information about the effective mass of ions.

2. Experimental Setup

To excite GAW in TCABR, we use the four strap antenna developed for the AW heating of the plasma [13]. Lower power is applied and the waves are detected with a pair of magnetic probes separated by the distance 25cm in toroidal direction. The scheme of our experimental setup is shown in figure 1, where we may observe two antenna modules composed of four straps each on opposite sides of the tokamak. In the presented experiments, we only use one strap of one antenna module to excite the GAW.

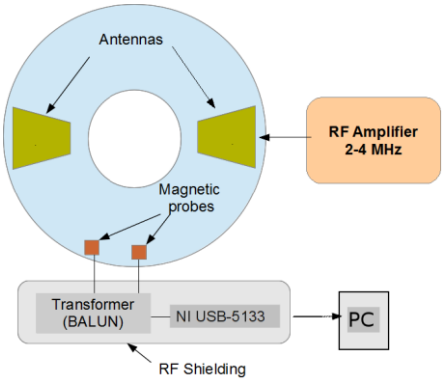

Figure 1. Schematic of the setup used for the experiments. Highlighting the principal equipment used for GAW excitation and detection.

Beyond the antenna, we have two magnetic probes, each probe may be used to measure the poloidal or toroidal magnetic field perturbations. Only the poloidal field is considered in the presented work. The RF antenna current is measured with a Rogowski coil. To collect the data we use a digitizer from National Instruments (NI) that transfers the collected raw data to the PC via USB connection. The amplifier used to feed the antenna is a class-D RF amplifier with MOSFET that operates in the frequency range 2-4 MHz.

2.1. Magnetic probes and BALUN

To measure the magnetic fields excited by the antenna in the plasma we use two poloidal magnetic probes [13] separated by a toroidal angle of approximately ~ 20° and on the same poloidal angle. The magnetic probe signal first goes through a BALUN (BALanced to UNbalanced transformer) [14] so we can ground one of the sides of the signal for measurement, the BALUN also works like a choke, eliminating common modes. The setup presented in figure 2 is also known as a choke BALUN. To digitize the signals we use two NI USB-5133 modules connected to a PC, this equipment is from National Instruments. We set the sampling frequency at 50MS/s, as we are interested in frequencies up to 4 MHz only, this gives sufficient number of points in a period for analyzes.

The PC, BALUN and NI USB-5133 are placed inside a shielded cabinet, so we have some kind of additional insulation from RF interference. The cables used to send the signals from the magnetic probes to the BALUN are BNO (twin-axial cabling).

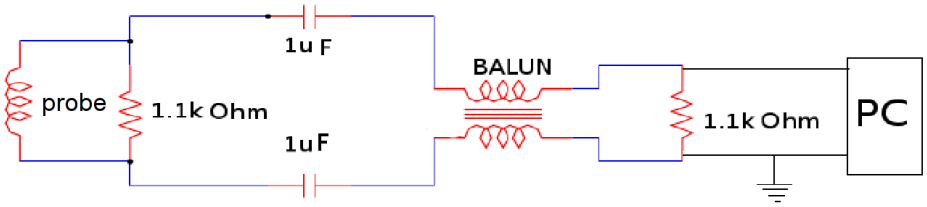

Figure 2. Schematic of the equipment use for measurement of magnetic probe signals.

The system has four input channels of 8 bits. Besides the probe signals, we also measured the antenna RF current using a Rogowski coil. There is care not to do ground loops as we use different systems, the use of the BALUN, as it is shown on the scheme figure 2, helps prevent it.

2.2. RF Amplifier and antennas

To induce the waves in the plasma we use a class-D RF amplifier with MOSFET, which operates in the frequency range 2-4 MHz it allows frequency scanning or fixed frequency currents. The amplitude of the RF current stays stable enough during ~20ms in the antenna with a Faraday screen. Each antenna set consists of four straps, two on top of the tokamak and two on the bottom, but only one strap was used to excite the waves in these experiments. The amplifier is a switching amplifier, and it needs an external function generator to switch the MOSFETs at the desired frequency to excite the GAW.

In figure 3, we present the time evolution of the RF current in the two different detection modes (fixed and swept frequencies). In the first case, gas injection is used to stimulate a ramp up of the plasma density, due to that the resonant condition may be met. In the second case, the density stays almost constant when the series of frequency sweeps of the RF current is induced.

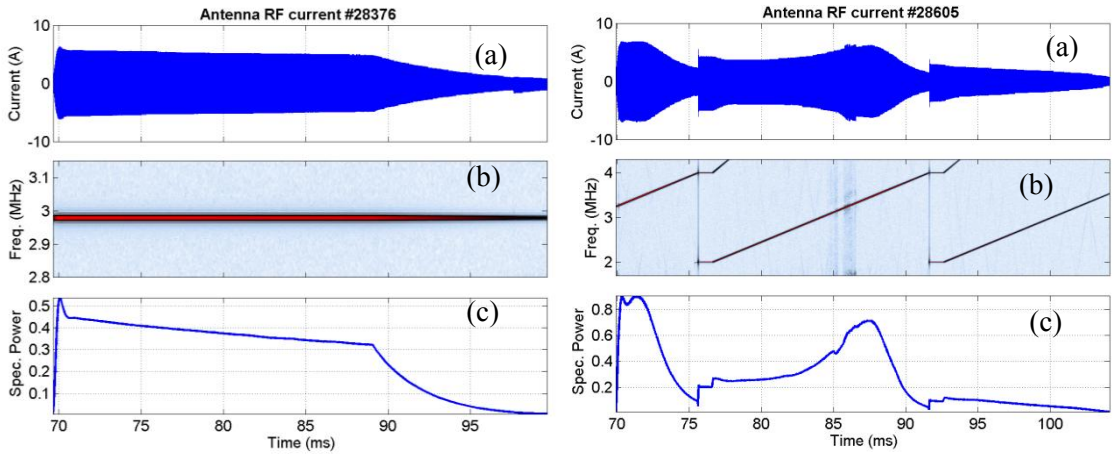

Figure 3. Typical characteristic of the RF current excited by the amplifier at the antenna. With fixed frequency (left) and frequency scanning (right). There is the raw data (a), the spectrogram (b) and spectral power on the RF frequency (c).

3. Results and Discussion

As it was mentioned the previous section, we used two methods to identify the resonances. To illustrate these methods, we selected two different shots that are typical for each case. The plasma parameters for each type of shots are shown in figure 4. In the shot #28376, a RF current of fixed frequency with a ramp up in the plasma density is used, while a sweep of the RF power frequency with a fixed plasma density is used in the shot #28605.

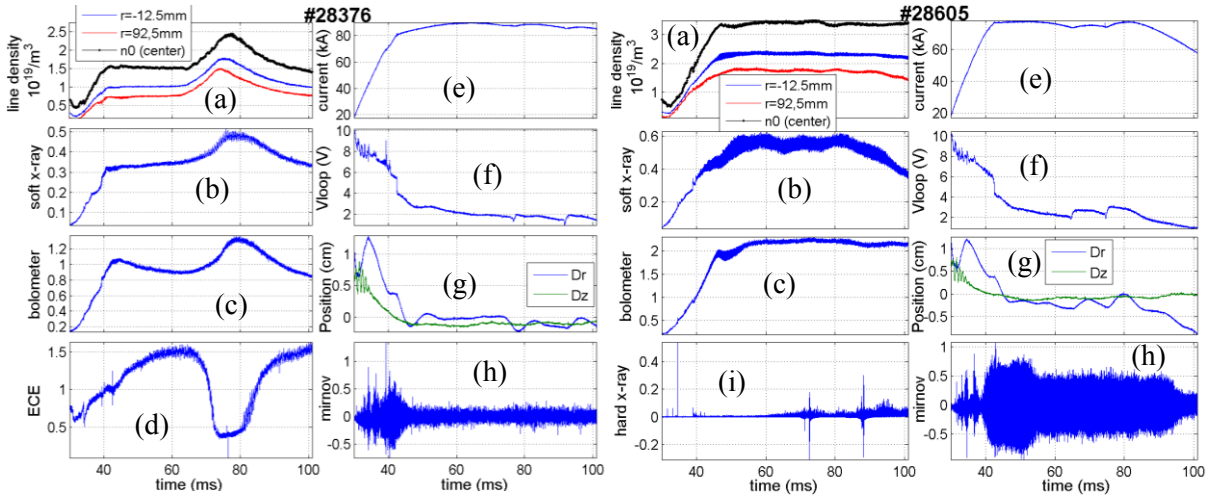

Figure 4. Basic plasma parameters for TCABR shots #28376 (left) and #28605 (right). The signals presented are the plasma electronic density (a), soft X-ray emission from core (b), bolometer signal from core, ECE signal (d), plasma current (e), loop voltage (f), plasma position (g), magnetic oscillations (h) and hard X-ray emission (i).

3.1. Shot #28376

We begin the discussion of RF experiments related to the shot #28376 shown in figure 4 (left) and the regime of the RF current to excite the GAW is presented in figure 3. In this case, gas injection is

performed in the middle of the discharge and RF power was applied during the formed density ramp up. Assuming a parabolic density profile $\propto n_0(1-r^2/a^2)^{\alpha}$, we calculate the density n_0 at the plasma center and the α-power using two line integrated density data from our interferometer. Those have the chord positions r=-1.25 and +9.25 cm with respect to the chamber center. It should be noted that the position of the plasma column was stable during the density ramp up and the estimated Shafranov shift is ~ 0.8 cm [15]. Due to that, we may adjust the central density and the α-parameter, those are necessary for A_{eff} in equation (1) because the GAW depends strongly on the central plasma density.

Using the respective probe measurements, in figure 5 we present the phase difference between the signals of the probes and the spectral power respective to the same frequency of the RF current. Two GAW resonances, one for the rising density and the other for the falling density, are identified by the abrupt changes in the phase and spectral power signals. The estimated density at the center of the plasma is the same for both resonances, $1.97\text{x}10^{13}/\text{cm}^3$ and $1.93\text{x}10^{13}/\text{cm}^3$ respectively, indicating the same kind of excited mode.

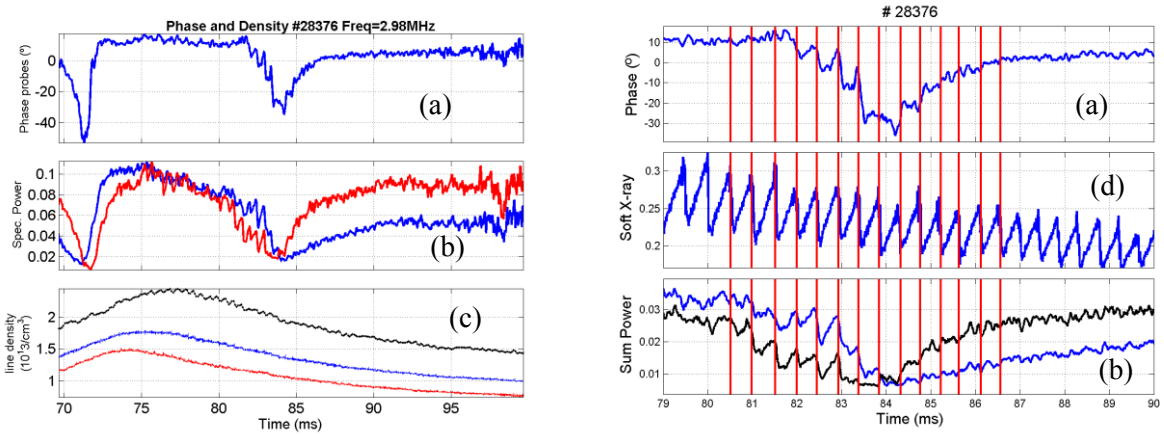

Figure 5. Probe signal for shot #28376 compared with the plasma electronic density (left) and with saw-tooth oscillations measured by soft X-ray (right). We have the phase between the probes (a) and their spectral power at the RF frequency (b), the electronic density measured by interferometer and estimation of central density (c) and saw-tooth oscillations measured by soft X-ray (d).

Beating of the probe signals by the strong saw-tooth (ST) oscillations measured with the soft x-ray diagnostic observed during the slow falling down density phase is shown in figure 5. Due to the slower variation, there are many saw-tooth oscillations that occur during the necessary time to pass the GAW resonant condition that reveals some specific details of the GAW resonances. We propose that this strong beating is related to the accumulation of impurities on the plasma core during the saw-tooth formation and its release after the saw-tooth crash [16]. The impurities accumulated on the plasma center changes the electron density and effective ion mass that consequently changes the GAW resonant frequency. This accumulation explains the beating, as well as the phase inversion of the saw-tooth oscillations at the minimum phase difference between the probes in figure 5. The phenomenon of the GAW frequency modulation had already been demonstrated in other experiments [7], but the phase inversion effect was not observed.

The ST phase inversion can be considered as the exact moment of the GAW resonant condition. Before that moment, the ST density rise gets closer to the GAW resonance, then, it abruptly moves away from the GAW resonant condition in each saw-tooth crash. After passing of the GAW resonance, situation is changed to inverse. Due to the ST effect and the localization of the q=1 position at $r \approx 4$ cm, we can expect that the GAW stays at the plasma core. Finally, the GAW mode numbers

may be identified as *N/M*=-2/-1 because this mode has the q-minimum position at the magnetic axes for the standard discharges in TCABR for monotonic q-profile in accordance with equation (1).

As it was earlier mentioned, the Pfirsch-Schlüter regime may causes an accumulation of impurities on the plasma core [9] changing the density profile equation (2). This accumulation creates a higher density at the plasma core, so a higher value for the effective ion mass on the center of the plasma should be expected. To confirm that, we compare the cut off density of the ECE signal that is at n_{cut}=2.22x10^{13}cm^{-3} with the one estimated from the interferometer data for the already mentioned parabolic profile n_0≈2.x10^{13}cm^{-3}. That indicates that the electronic density may have a "Mexican hat" profile [16,17] due to impurity accumulation. Using the density value n_0=2.22x10^{13}cm^{-3}, we estimate A_{eff}≈1.36 with 10% relative error. To complete this analysis for the impurity composition (carbon + iron), we use scaling law of the old TCA [10].

$$Z_{eff}(0) = 1.84 \times 10^{-4}\left(T_{e0}^{1,5} V_{Loop}/B_T\right) - 0.755 \qquad (3)$$

Where T_{e0}≈480eV is the plasma temperature at the center, V_{loop}≈1.8V the loop voltage and B_T=1.07T the toroidal magnetic field. Using equation (3) we calculate Z_{eff}=2.5 for the data of discharge #28376. Finally, that gives us A_{eff}=1.34 considering 3% of light ion impurities (totally striped carbon), and 0.4% of heavy ion impurities, that is, iron (Fe^{+15}) in our case.

3.2. Shot#28605

Another method to excite the GAW modes is shown on figure 6. In this case, we try to maintain a flat plasma density together with the frequency sweeps from 2-4 MHZ lasting 15 ms. Opposed to the other shot, in this one we try to maintain the plasma density as flat as possible. The respective RF current used to excite the modes is shown in the right panel of figure 3 and the basic plasma parameters from this shot can be seen on the right panel of figure 4.

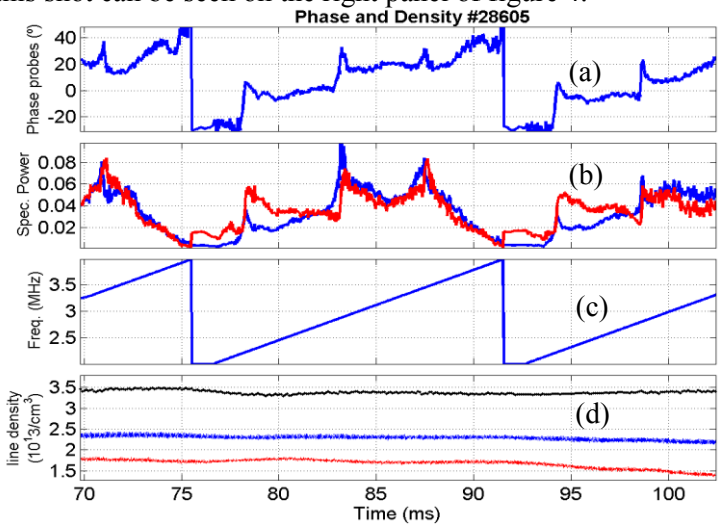

Figure 6. Time traces of the phase difference (a), spectral power (b) of the probe signals in comparison with the frequency sweeps (c) of the RF antenna current and the plasma electronic density (d) in the shot #28605.

The result of the signal treatment similar to the previous case is presented in figure 6. We can observe three distinct resonant spikes in the phase difference and spectral power of the probe signals during one sweep (75.4-91.5 ms). Each identified resonance corresponds to a different GAW mode number. Different from shot #28376, we cannot observe the beating with saw-tooth oscillations in figure 6 because the sweeping time for the frequency range is too fast to resolve the ST period.

3.3. Data obtained from series of shots

In figure 7, we present a summary of the GAW frequency dependence from central electronic density, based on data collected from about 50 shots with detected GAW resonances. The GAW modes form four distinct groups, due to different combination of the toroidal and poloidal mode numbers (*N/M*), and in each group the frequencies are inversely proportional to the square root of the density, as it comes from equation (1). It is difficult to get the spectrum of the higher frequencies, as we have large number of *M/N* combinations to satisfy the obtained data.

The presented data in figure 7 are fed with error bars from the measurements, we estimated an error of about 4% for the central density and 30 kHz for the frequency value. Regarding the mode numbers of the data presented, the lower blue mode should be the mode *N/M*=-1/-1, as this is the lowest possible mode number [1, 2]. The mode marked by the red dots has *N/M*=-2/-1 as mode numbers, the identification is due to the ST localization at the plasma center and its beating with the magnetic probe data, as explained previously. Identification of other modes is doubtful, because there are more than one combination of *N/M* that set the experimental data, and what we can say is only the most probable *N+M* combination for each specific band. This way we have *N+M*=-2 (blue), *N+M*=-3 (green), *N+M*=-4 (wine) and *N+M*=-5 (pink).

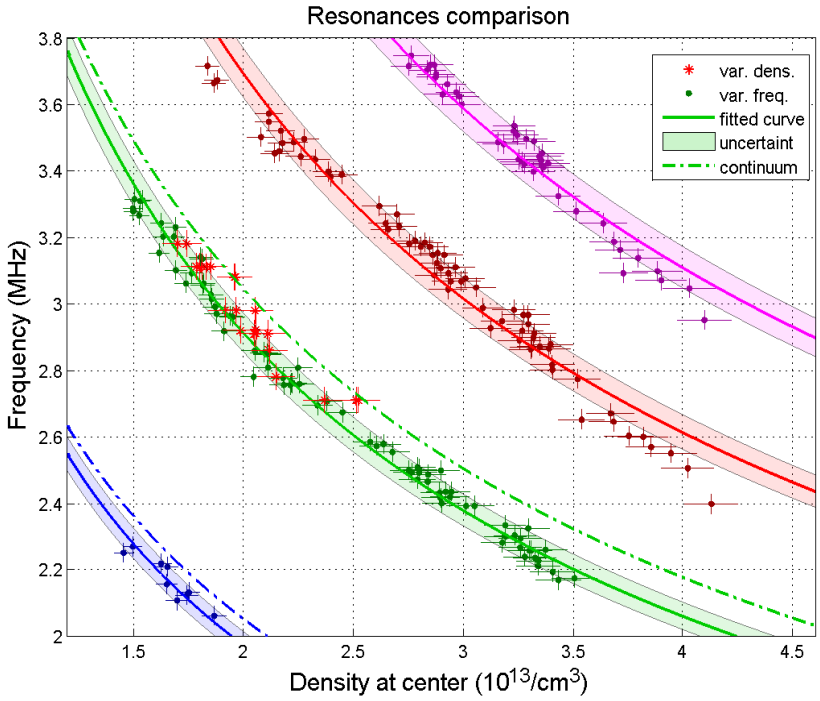

Figure7. Summary of identified resonant frequencies over the estimated density at the center of the plasma for resonances with N+M equals to -2 (blue), -3 (green), -4 (red) and -5 (pink). The dot-dash lines represent the Alfvén continuum minimum for effective mass number A=1.36 and density 1.15 times higher as the value shown on axis *N/M*=-1/-1 (blue) and -2/-1 (green).

The theoretical dependence of the frequency from density from equation (1) is also plotted (dash-dot lines) for the *N/M*=-1/-1 (blue) and -2/-1 (green) modes. The effective ion mass used was of

A_{eff}=1.36, taking into account 13% correction of the central density value, as we have found from ECE cut off for the shot #28376.

Furthermore, we note that the GAW frequency relation with the density is the same for the density ramp or frequency scan methods. It can be seen for the N+M=3 modes in figure 7 that the respective data points marked by the red stars and green dots statistically coincide. As well, we note that there is the distance $\Delta\omega/\omega_A \approx$2-5% between the continuum and main frequency for the *N/M*=-2/-1 eigenmode [1, 2, 18], this distance depends on Hall effect and magnetic shear.

4. Conclusion

The experiments with the low RF power excitation of the GAW and their detection by the magnetic probes in TCABR confirm that it may be a very effective method for diagnostics for the ion effective mass. Using the magnetic probes, we can identify the GAW resonances in TCABR and their behavior is found to be predicted by the Alfvén continuum equation (1). Also, it is demonstrated that there is no difference in results in identification of the GAW resonances excited by the fixed frequency during the density ramp up or RF current frequency sweep methods. The typical mass number is estimated to be at A_{eff}=1.36 and Z_{eff}=2.5, this corresponds to a mixture of 3% of the full stripped carbon impurities and 0.3% of iron Fe^{+15} impurities. For better results, it is necessary additional information of the central density detected by other diagnostics, and it should be noted that the presented method for A_{eff} identification is very sensitive to the considered value of the plasma density.

Acknowledgements

This work was supported by FAPESP (Research Foundation of the State of São Paulo), grant 2011/50773-0.

References

[1] Appert K, Gruber R, Troyuon F and Vaclavik J 1982 Excitation of global eigenmodes of the Alfven wave in Tokamaks *Plasma Phys.* **24** 1147

[2] Ross D W, Chen G L and Mahajan S M 1982 Kinetic description of Alfvén wave heating *Phys. Fluids* **25**, 652

[3] Evans T E et al 1984 Direct Observation of the Structure of Global Alfvén Eigenmodes in a Tokamak Plasma *Phys. Rev. Lett.* **53** 1743- pretex

[4] Collins G A, Hofmann F, Joye B, Keller R, Lietti A, Lister J B and Pochelon A 1986 The Alfvén wave spectrum as measured on a tokamak *Physics of Fluids* **29**, 2260-2272

[5] Holties H A, Fasoli A, Goedbloed J P, Huysmans G T A and Kerner W 1997 Determination of local tokamak parameters by magnetohydrodynamic spectroscopy, *Phys. Plasmas* **4**, 709-719

[6] Fasoli A, Dobbing A, Gormezano C, Jacquinot J, Lister J B, Sharapov S E and Sibley A 1996 Alfven eigenmode excitation by ICRH beat waves, *Nucl. Fusion*, **36**, 258

[7] Collins G A, Howling A A, Lister J B and Marmillod P 1987 Central mass and current density measurements in Tokamaks using the discrete Alfven wave spectrum *Plasma Phys. Control. Fusion* **29** 323

[8] Descamps P, Wassenhove1 G, Koch R, Messiaen A M and Vandenplas P E 1990 Determination of central q and effective mass on textor based on discrete Alfvén wave (DAW) spectrum measurements *Phys. Lett.* A, **143**, 311

[9] Elfimov A G, Ruchko L F, Galvão R M O,Elizondo J I, Sanada E, Kuznetsov Y, Fagundes A N, de Sá W P, Varandas C A F, Manso M E C, Varela P, Silva A, Ivanov A A 2006 Identification of local Alfvén wave resonances with reflectometry as a diagnostic tool in tokamaks *Nucl. Fusion* **46** S722

[10] De Chambrier A, Collins G A, Hollenstein C, Joye B, Lister J B, Moret, J-M, Nowak S,

Pochelon A and Simm W 1984 *Target plasma conditions in TCA* Center for Research In Plasma Physics, École polytechnique fédérale de Lausanne
[11] Fussmann G, Field A R, Kallenbach A, Krieger K, Steuer K -H and The ASDEX Team 1991 *Plasma Phys. Control. Fusion* **33** 1677
[12] Ruchko L F, Ozono E, Galvão R M O, Nascimento I C, Degasperi F T and Lerche E 1998 Advanced antenna system for Alfvén wave plasma heating and current drive in TCABR tokamak. *Fusion Engineering and Design* **43** 15
[13] Lerche E 2003 *Aquecimento do plasma por ondas de Alfvén no tokamak TCABR*, . Universidade de São Paulo: Instituto de Física. online: http://www.teses.usp.br/teses/disponiveis/43/43134/tde-17072012-141903/.
[14] Sevick J 2006 *Transmission Line Transformers* (Raleigh: Scitech Publishing)
[15] Pereverzev G, Yushmanov P N 2002 Astra Automated System for Transport Analysis in a Tokamak *IPP-Report* 5/98 Max-Plank-Institute für Plasmaphysik
[16] Nicolas T, Sabot R, Garbet X, Lütjens H, Luciani J -F, Guimaraes-Filho Z, Decker J and Merle A 2012 *Phys. Plasmas* **19** 112305
[17] Nicolas T, Sabot R, Garbet X, Lütjens H, Luciani J -F, Sirinelli A, Decker J, Merle A and JET-EFDA Contributors 2013 Particle Flow during Sawtooth Reconnection: Numerical Simulations of Experimental Observations *Plasma and Fusion Research* **8** 2402131
[18] Amarante-Segundo G, Elfimov A G, Galvão, R M O, Ross D W and Nascimento I C 2001 Calculations of Alfvén wave driving forces, plasma flow, and current drive in the Tokamak Chauffage Alfvén wave experiment in Brazil (TCABR) *Phys. Plasmas* **8** 210